Supporting Information

Davis et al. 10.1073/pnas.1502264112

SI Materials and Methods

Reagents. Insulin, transferrin, and selenite (ITS) media supplement was purchased from Sigma Aldrich. Milk and serum total Ca^{2+} levels were measured using the QuantiChrom Ca^{2+} Assay Kit (BioAssay Systems), and protein was measured using the Dc Protein Assay Kit (BioRad). QIAshredder Homogenizer Columns, RNeasy Plus Mini Kits, and Omniscript RT Kits were purchased from Qiagen. CellTracker (Orange CMRA and Green CMFDA) and Alexa Fluor 633 Phalloidin were purchased from Life Technologies. Immunomagnetic negative selection of mouse mammary epithelial cells was performed using the EasySep Mouse Epithelial Cell Enrichment Kit from Stem Cell Technologies. The following TaqMan Gene Expression Assays were purchased from Applied Biosystems: *Orai1* (Mm00774349_m1), *Orai2* (Mm04214089_s1), *Orai3* (Mm01612888_m1), *Stim1* (Mm01158413_m1), *Stim2* (Mm01223103_m1), and *Oxtr* (Mm01182684_m1).

Genotyping Primers. Genotyping was performed on mouse tail DNA by PCR using the following primers and reaction conditions: to distinguish $Orai1^{+/+}$ (488 bp), $Orai1^{+/-}$, and $Orai1^{-/-}$ (300 bp), 5′-TCA CGC TTG CTC TCC TCA TC-3′, 5′-TAA GGG CGA CAC GGA AAT G-3′, and 5′-AGG TTG TGG ACG TTG CTC AC-3′; to distinguish the *Orai1* floxed (360 bp) and WT (220 bp) alleles, 5′-CAG CGT GCA TAA TAT ACC TAA CTC TAC CCG-3′ and 5′-GTA TTG ATG AGG AGA GCA AGC GTG AAT C-3′; to distinguish Cre positivity (100 bp), 5′-GCG GTC TGG CAG TAA AAA CTA TC-3′ and 5′-GTG AAA CAG CAT TGC TGT CAC TT-3′; and PCR positive controls, 5′-CTA GGC CAC AGA ATT GAA AGA TCT-3′ and 5′-GTA GGT GGA AAT TCT AGC ATC ATC C-3′.

Single-Cell Ca^{2+} Measurements. Mammary luminal and myoepithelial cells were plated on collagen-coated glass coverslips and allowed to attach overnight in mammary growth medium, containing DMEM/F12 (1:1), FBS (5%), ITS media supplement, gentamicin (50 μg/mL), penicillin (100 U/mL), and streptomycin (100 μg/mL) (1). Cells were loaded with fura-5F (1 μM) for 30 min at 37 °C and washed with HBSS (NaCl 120 mM, KCl 5.4 mM, $MgCl_2$ 0.8 mM, Hepes 20 mM, glucose 11 mM, and $CaCl_2$ 2 mM). For intracellular Ca^{2+} measurements, cells were bathed in HBSS and fluorescence images were recorded and analyzed with a digital fluorescence imaging system (2). For assessing SOCE, cells were bathed in nominally Ca^{2+}-free HBSS supplemented with BAPTA (500 μM) for 2 min and treated with TG (2 μM) to deplete ER Ca^{2+} stores, before Ca^{2+} readdition (2 mM). Changes in intracellular Ca^{2+} are expressed as the ratio of fura-5F fluorescence (F340/380) and were corrected for autofluorescence. R_{max} averaged 12.2 for mammary epithelial cells, whereas peak ratio values for oxytocin and TG were less than 5, indicating that the ratio values were substantially less than saturation and thus essentially proportional to the Ca^{2+} concentration.

Real-Time RT-PCR. For quantitative analysis of gene expression in the mammary gland, mammary tissue was excised from euthanized female mice and immediately frozen in liquid nitrogen. Tissue disruption was performed using a mortar and pestle followed by homogenization with QIAshredder homogenizer columns. Total RNA from tissue or FACS-sorted cell lysates was purified using the RNeasy Plus Mini Kit, with gDNA Eliminator columns to remove any contaminating genomic DNA (3). Reverse transcription was performed using the Omniscript RT Kit, and resulting cDNA was amplified with an Applied Biosystems 7500 Fast Real-time RT-PCR machine, using TaqMan Fast Universal PCR Master Mix and TaqMan Gene Expression Assays. Relative quantification was calculated with reference to 18S ribosomal RNA and analyzed using the comparative C_T method (4).

Histology and Whole-Mount Analysis. Mammary tissue was prepared for whole-mount analysis as previously described (5). Briefly, mammary tissue was excised from euthanized female mice and spread on wide microscope slides. Tissue was fixed overnight in Carnoy's Fixative [ethanol (60%), chloroform (30%), and glacial acetic acid (10%)], rehydrated through graded ethanol washes, stained with carmine alum stain [carmine (0.2%) and aluminum potassium sulfate (0.5%)] overnight, and dehydrated with graded ethanol washes. Tissue was cleared in xylene for 48 h (5) and mounted with Permount Mounting Medium. Images were acquired using a Zeiss stereo microscope.

For fluorescence whole-mount analysis, mammary tissue from lactating mice was removed and dissected into 1–2-mm^3 pieces. Tissue was fixed in neutral buffered formalin (4%), rinsed in PBS, and transferred to PBS containing sodium azide (0.05%). Tissue was opened using Triton-X 100 (1%) in PBS-azide for 18 h, stained with phalloidin, and imaged using a Zeiss 780 laser scanning microscope (6).

For 5-bromo-4-chloro-3-indolyl-β-galactosidase (X-gal) staining, tissue was processed as described for fluorescence whole-mount analysis, but after opening with Triton-X 100, tissue pieces were transferred to X-gal staining solution [$MgCl_2$ (2 mM), potassium ferricyanide (4 mM), potassium ferrocyanide (4 mM), X-gal (1 mg/mL) in PBS] overnight at 37 °C. Tissue pieces were embedded in paraffin and sectioned at 15 μm.

For histological examination, the right inguinal mammary gland was excised and fixed in neutral buffered formalin (10%) for 48 h. Tissue was embedded in paraffin, sectioned at 5 μm, and stained with H&E.

Statistics. Statistical analysis was performed using GraphPad Prism for Windows (v6.03). Statistical tests used for each study are indicated in the figure legends.

1. Mroue R, Bissell MJ (2013) Three-dimensional cultures of mouse mammary epithelial cells. *Methods Mol Biol* 945:221–250.
2. Xing J, et al. (2014) Role of Orai1 and store-operated calcium entry in mouse lacrimal gland signalling and function. *J Physiol* 592(Pt 5):927–939.
3. Davis FM, et al. (2014) Induction of epithelial-mesenchymal transition (EMT) in breast cancer cells is calcium signal dependent. *Oncogene* 33(18):2307–2316.
4. Suchanek KM, et al. (2002) Peroxisome proliferator-activated receptor alpha in the human breast cancer cell lines MCF-7 and MDA-MB-231. *Mol Carcinog* 34(4):165–171.
5. Davis BJ, Fenton SE (2013) The mammary gland. *Haschek and Rousseaux's Handbook of Toxicologic Pathology*, eds Haschek WM, Rousseaux CG (Academic Press, Wallig, MA), pp 2665–2694.
6. Haaksma CJ, Schwartz RJ, Tomasek JJ (2011) Myoepithelial cell contraction and milk ejection are impaired in mammary glands of mice lacking smooth muscle alpha-actin. *Biol Reprod* 85(1):13–21.

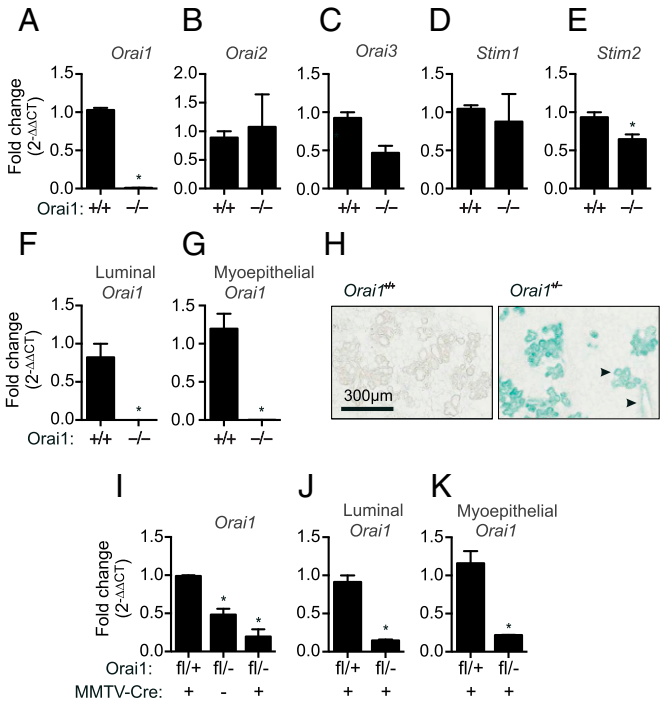

Fig. S1. Gene expression in mammary glands of Orai1 KO mice. (*A–E*) mRNA levels of *Orai* and *Stim* isoforms in mammary glands of $Orai1^{+/+}$ and $Orai1^{-/-}$ mice, and *Orai1* expression in sorted luminal (*F*) and myoepithelial (*G*) cells ($n = 3–4$ mice). (*H*) X-gal staining for the detection of the Orai1–β-galactosidase fusion protein in alveoli (left arrow) and ducts (right arrow) of mammary tissue from lactating $Orai1^{+/+}$ and $Orai1^{+/-}$ mice ($n = 2–3$ mice). (*I*) Orai1 mRNA levels in mammary tissue from cKO or control mice and in sorted luminal (*J*) and myoepithelial (*K*) cells ($n = 3–4$ mice). Data represent mean ± SEM; $P < 0.05$, Student's *t* test (*A–G*, *J*, and *K*) or one-way ANOVA with Bonferroni posttests (*I*).

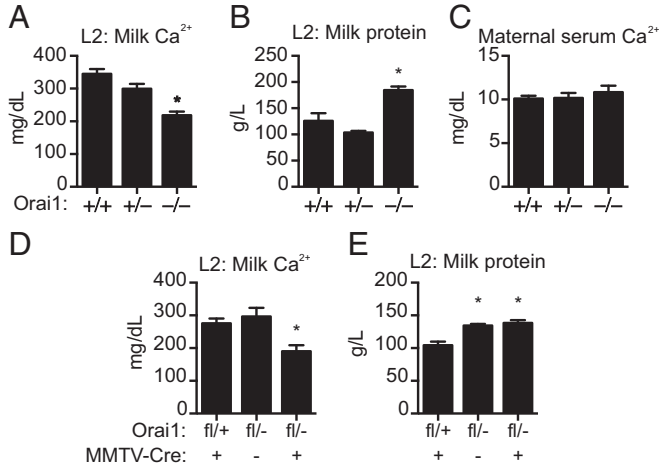

Fig. S2. Milk Ca^{2+} and maternal serum Ca^{2+} levels in Orai1 KO mice. (*A* and *B*) Total Ca^{2+} and protein concentrations in mouse milk collected from day 2 lactating (L2) $Orai1^{-/-}$ mice versus control genotypes ($n = 3$). (*C*) Maternal serum total Ca^{2+} levels in $Orai1^{-/-}$ mice versus control genotypes ($n = 3$). (*D* and *E*) Total Ca^{2+} and protein concentrations in mouse milk collected from day 2 lactating cKO mice versus control genotypes ($n = 3–4$). Data represent mean ± SEM; *$P < 0.05$, one-way ANOVA with Bonferroni posttests.

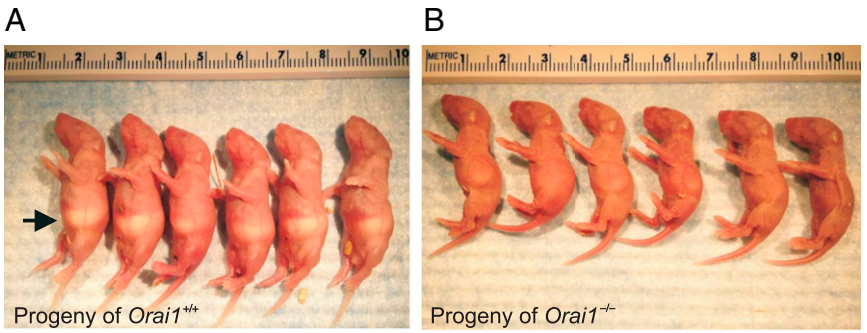

Fig. S3. Absence of milk spots in pups nursed by *Orai1*$^{-/-}$ dams. Pups nursed by (*A*) *Orai1*$^{+/+}$ and (*B*) *Orai1*$^{-/-}$ dams on PND4; arrow shows milk spots in pups nursed by *Orai1*$^{+/+}$ lactating dams.

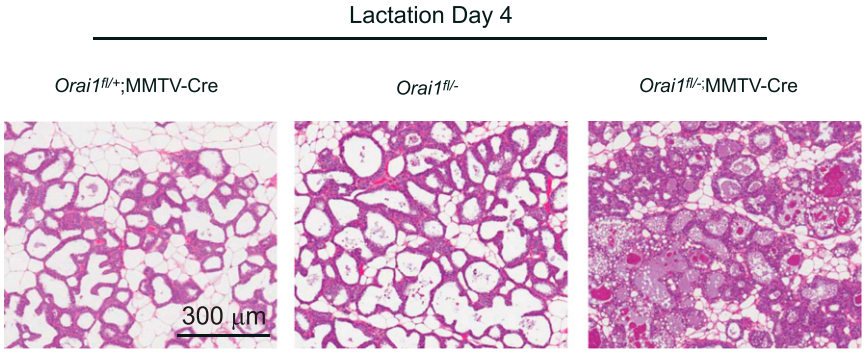

Fig. S4. Histological analyses of mammary glands from lactating mice with conditional deletion of Orai1 in the mammary gland. H&E-stained sections of mammary glands from Orai1 cKO mice (*Orai1*$^{fl/-}$;MMTV-Cre) or control genotypes on day 4 of lactation (n = 3 mice). (Scale bar, 300 μm.)

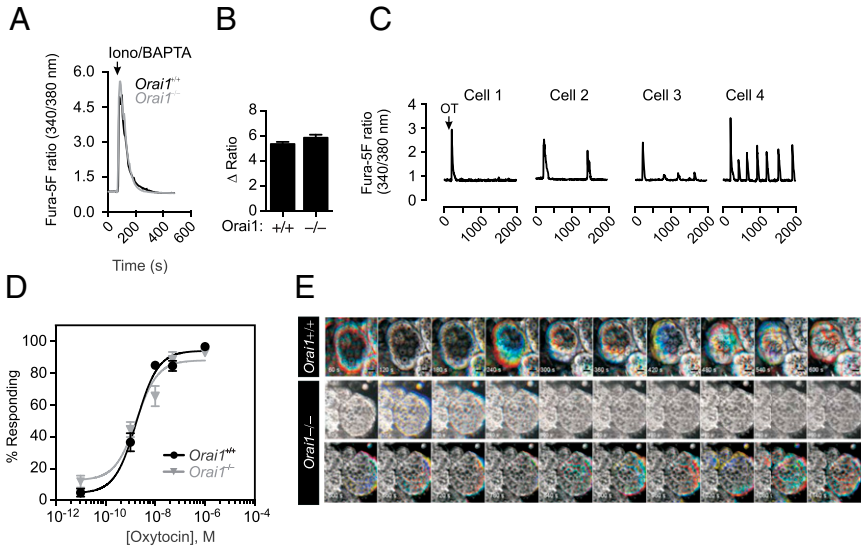

Fig. S5. Ca^{2+} homeostasis and signaling in myoepithelial cells and alveolar unit contraction. (*A*) Mobilizable intracellular Ca^{2+} stores in *Orai1*$^{+/+}$ (n = 151 cells) or *Orai1*$^{-/-}$ (n = 88 cells) myoepithelial cells treated with ionomycin (iono, 10 μM) in the absence of Ca^{2+} (BAPTA, 3 mM) and (*B*) peak ratio response (50–100 s). (*C*) Example traces of oxytocin-induced Ca^{2+} oscillations in wild-type cells. (*D*) Concentration–response relationship for oxytocin in terms of the percentage of cells responding with an elevation in cytosolic Ca^{2+} throughout the assay (n = 3 coverslips). (*E*) Visual representation of the spatial properties of alveolar unit contraction in *Orai1*$^{+/+}$ and *Orai1*$^{-/-}$ mammary glands. White areas represent no movement (*Materials and Methods*). $P > 0.05$, Student's t test.

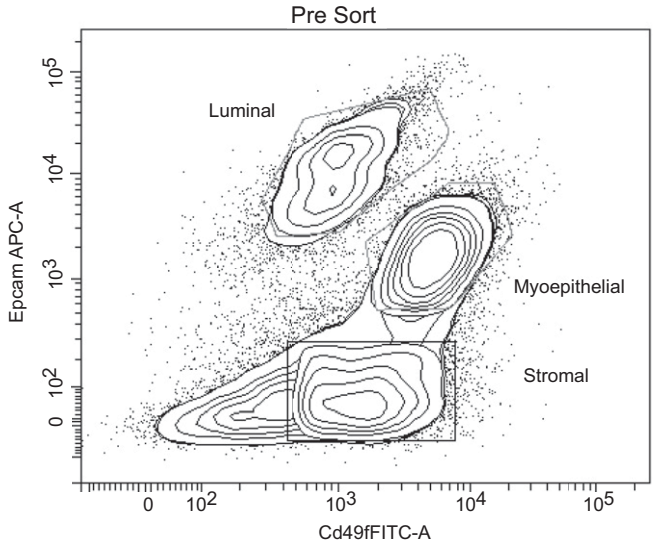

Fig. S6. Flow cytometric analysis of isolated mouse mammary cells. Example of flow cytometric analysis showing the gating strategy used to identify populations of viable luminal and myoepithelial cell types for cell sorting (*Materials and Methods*).

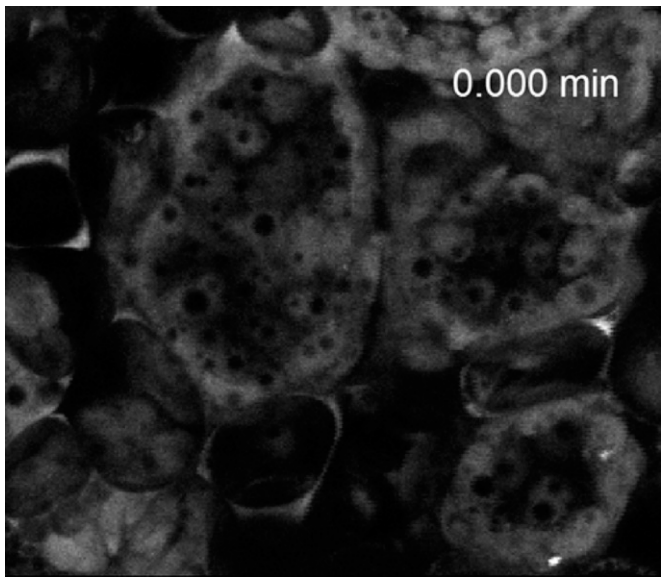

Movie S1. Alveolar unit contraction in response to oxytocin (50 nM) in mammary tissue pieces isolated from *Orai1*$^{+/+}$ mice.

Movie S1

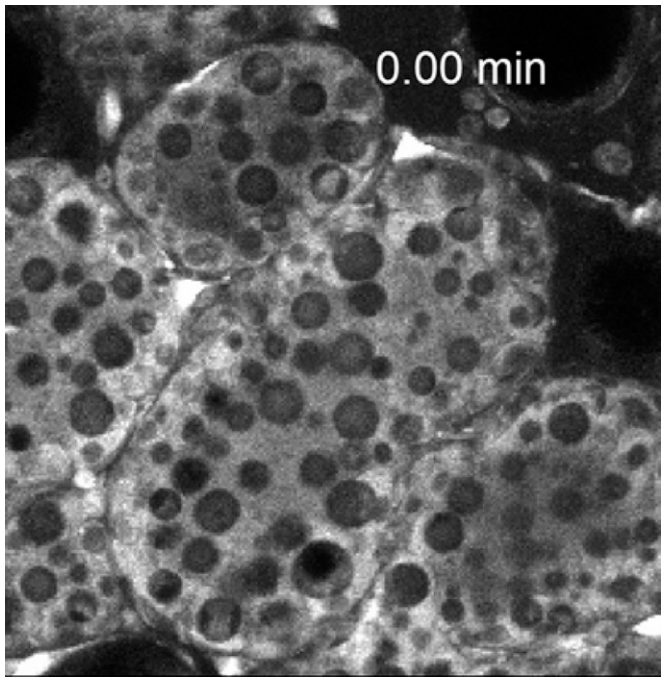

Movie S2. Alveolar unit contraction in response to oxytocin (50 nM) in mammary tissue pieces isolated from *Orai1*$^{-/-}$ mice.

Movie S2